

# Ion Exchange in Catanionic Mixtures: From Ion Pair Amphiphiles to Surfactant Mixtures

Eva Maurer, Luc Belloni, Thomas Zemb, and David Carrière\*

LIONS (Laboratoire Interdisciplinaire sur l'Organisation Nanométrique et Supramoléculaire),  
CEA/Saclay, F-91191 Gif-sur-Yvette Cedex, France

Received January 22, 2007. In Final Form: March 29, 2007

We have studied concentrated equimolar mixtures of tetradecanoic acid (myristic acid,  $C_{13}COOH$ ) and hexadecyltrimethylammonium hydroxide (CTAOH) in which the  $OH^-$  counterions are gradually exchanged by other anions ( $Cl^-$ ,  $Br^-$ ,  $CH_3COO^-$ ,  $CH_3-(C_6H_4)-SO_3^-$ ). We demonstrate that the stability of a  $L_\beta$  phase can be achieved at equimolarity between both surfactants, provided that the phase contains also a sufficient number of anions exchanged with  $OH^-$ . In the absence of exchange (equimolar mixture of  $C_{13}COOH$  and CTAOH), a three-dimensional crystalline  $L_c$  phase is produced. As the  $OH^-$  ions are replaced by other ions, a swollen  $L_\beta$  lamellar phase appears, first in coexistence with the  $L_c$  ( $D^* = 400 \text{ \AA}$ ) and then in coexistence with a dilute phase only ( $D^* = 215 \text{ \AA}$ ). In the latter regime, the repeating distance depends very little on the exchange ratio, but rather on the nature of the counterion. If too many  $OH^-$  ions are exchanged, the  $L_\beta$  phase becomes unstable again. A Poisson–Boltzmann model with charge regulation computed for a closed system predicts qualitatively the existence of this narrow domain of stability for the  $L_\beta$  phase.

## Introduction

Mixtures of surfactants of opposite charge, also called “catanionic” mixtures, have motivated a broad interest from the scientific community for different reasons.<sup>1,2</sup> For instance, dilute mixtures of surfactants are known to form thermodynamically stable vesicles,<sup>3</sup> the stability of which arises from the highly nonideal mixing between the surfactants.<sup>4</sup> These stable catanionic vesicles show potential applications in drug delivery devices and microreactors.<sup>5,6</sup> The highly synergetic effects between surfactants of opposite charge have also been used for the supramolecular synthesis of biologically active compounds<sup>7</sup> and for the enhancement of bioavailability by solubilization of fatty acids.<sup>8</sup> The study of catanionic aggregates is also helpful for addressing fundamental questions about self-assembly. The phase diagrams have been discussed in terms of force balance,<sup>9–11</sup> and the morphology of the aggregates themselves require inspection of the curvature, rigidity, and crystalline state, i.e., molten or solid, of the bilayer itself.<sup>12,13</sup>

In most of these systems, each ionic surfactant is accompanied by its own counterion in solution. One particular catanionic system consists of a mixture of surfactants in which the organic or inorganic counterions of the surfactants are absent, preventing

electrostatic screening upon surfactant association.<sup>2,14,15</sup> In the myristic acid/cetyltrimethylammonium hydroxide/water system, a rich polymorphism has been reported, with lamellar phases,<sup>16</sup> discs,<sup>17</sup> or faceted vesicles<sup>18</sup> depending on the composition. The peculiar morphologies in this system originate from the lateral segregation of the surfactants, leading to a cocrystallization in the membrane and rejection of the excess surfactants into defects such as pores or rims.<sup>12</sup> It has been argued that the use of  $H^+$  and  $OH^-$  as the initial surfactant counterions allows recombination into water and thus the absence of salt in solution. The resulting large Debye length would allow electrostatics to be the driving force for this in-plane segregation since typical electrostatic pair potentials would become of the order of  $kT$ .

As already underlined by Tondre and Caillet,<sup>2</sup> this illustrates a fundamental difference between “surfactant mixtures”, where salt is released from the combination of surfactants, as opposed to “ion pair amphiphiles” where the salt is eliminated or intrinsically absent. In this paper, we study the transition from one situation to the other. A myristate/cetyltrimethylammonium ion pair amphiphile is progressively converted into a surfactant mixture by exchanging the  $OH^-$  anions with other  $X^-$  anions, all other parameters remaining unchanged. We first demonstrate experimentally that the introduction of  $X^-$  anions promotes the stability of lamellar phases in a narrow domain of composition. We then compare the experimental results with a Poisson–Boltzmann model with charge regulation in a closed system. The qualitative agreement between the experiments and the model allows general conditions for the stabilization of catanionic phases by ion exchange to be proposed.

## Materials and Methods

Myristic acid (Fluka) was recrystallized twice from hot acetonitrile. A 10% weight solution of CTAOH in water (Sigma) was freeze-

\* To whom correspondence should be addressed. E-mail: david.carriere@cea.fr. Tel.: +33 1 69 08 54 89. Fax: +33 1 69 08 66 40.

(1) Khan, A.; Marques, E. *COCIS* **1999**, 4, 402.  
(2) Tondre, C.; Caillet, C. *Adv. Colloid Interface Sci.* **2001**, 93, 115.  
(3) Kaler, E.; Murthy, A.; Rodriguez, B.; Zasadzinski, J. *Science* **1989**, 245, 1371.  
(4) Safran, S.; Pincus, P.; Andelman, D. *Science* **1990**, 248, 354.  
(5) Caillet, C.; Hebrant, M.; Tondre, C. *Langmuir* **2000**, 16, 9099.  
(6) Yaacob, I.; Nunes, A.; Bose, A.; Shah, D. *J. Colloid Interface Sci.* **1994**, 168, 289.  
(7) Blanzat, M.; Perez, E.; Ricco-Lattes, I.; Prome, D.; Lattes, A. *Langmuir* **1999**, 15, 6163.  
(8) Douliez, J. P.; Navailles, L.; Nallet, F. *Langmuir* **2006**, 22, 622.  
(9) Jokela, P.; Jonsson, B.; Khan, A. *J. Phys. Chem.* **1987**, 91, 3291.  
(10) Brasher, L.; Herrington, K.; Kaler, E. *Langmuir* **1995**, 11, 4267.  
(11) Shiloach, A.; Blankschtein, D. *Langmuir* **1998**, 14, 1618.  
(12) Dubois, M.; Lizunov, V.; Meister, A.; Gulik-Krzywicki, T.; Verbavatz, J. M.; Perez, E.; Zimmerberg, J.; Zemb, T. *PNAS* **2004**, 101, 15082.  
(13) Coldren, B.; Warriner, H.; van Zanten, R.; Zasadzinski, A. *Langmuir* **2006**, 22, 2474.

(14) Hao, J.; Liu, W.; Xu, G.; Zheng, L. *Langmuir* **2003**, 19, 10635.  
(15) Zemb, T.; Dubois, M. *Aust. J. Chem.* **2003**, 56, 971.  
(16) Dubois, M.; Gulik-Krzywicki, T.; Demé, B.; Zemb, T. *C. R. Acad. Sci. Paris II C* **1998**, 1, 567.  
(17) Zemb, T.; Dubois, M.; Demé, B.; Gulik-Krzywicki, T. *Science* **1999**, 283, 816.  
(18) Dubois, M.; Demé, B.; Gulik-Krzywicki, T.; Dedieu, J. C.; Vautrin, C.; Désert, S.; Perez, E.; Zemb, T. *Nature* **2001**, 411, 672.

dried, recovered in a minimum amount of ethanol (typically 1 mL for 5 g), and recrystallized from anhydrous ether. The solid was dried under a stream of nitrogen. This recrystallization has to be performed to eliminate products of self-decomposition of CTAOH, mainly trimethylamine and hexadecene resulting from Hoffmann elimination. All other products (CTABr, CTACl, HCl, HBr, acetic acid, and paratoluenesulfonic acid) were purchased from Sigma and used as such.

Catanionic mixtures of myristic acid, CTAOH, and CTAX ( $X^- = \text{Cl}^-, \text{Br}^-, \text{CH}_3\text{COO}^-$ , or  $\text{CH}_3-(\text{C}_6\text{H}_4)-\text{SO}_3^-$ ) were prepared by stirring the appropriate amounts of surfactants, optionally acids HX, and Milli-Q water at 50 °C at least overnight, heating at 60 °C for 1 min, and cooling down at room temperature. Introduction of the  $X^-$  counterion was performed by using either directly CTAX or the corresponding acid HX in the preparation. Both procedures gave identical results in terms of interlamellar distances and surfaces per chains.

Small-angle and wide-angle X-ray scattering experiments (SAXS and WAXS) were performed using a homebuilt pinhole-geometry camera<sup>19</sup> and recorded on an image plate. The SAXS setup was used to measure the distances between the layers from the 00*k* Bragg reflections with a typical exposure time of 1 h. The WAXS setup was used to detect any  $L_c$  phase from the 001 reflection at  $0.19 \text{ \AA}^{-1}$  and/or a series of peaks at wider angles ( $1.4 \text{ \AA}^{-1}$ – $1.6 \text{ \AA}^{-1}$ ) with a typical exposure time of 10 h.

A Poisson–Boltzmann model with charge regulation boundary conditions<sup>20</sup> and imposed overall composition in the surfactant mixture solution + excess water finite “reservoir” of known respective volumes was used to compute the repulsions between the  $L_\beta$  lamellae in coexistence with a dilute phase. By contrast to other previous models,<sup>21</sup> neither the concentration of ion pairs is imposed in each phase nor their chemical potential, but only the overall composition in the global system. This situation is intermediate between canonical and grand-canonical conditions. The lamellar phase is modeled as parallel, charged planes separated by a medium of uniform dielectric constant ( $\epsilon = 78$  at 293 K). The dissociations of myristic acid and CTAOH are given by the local laws of mass action, i.e., are determined by the  $\text{pK}_a$ 's and the concentrations of  $\text{H}^+$  and  $\text{OH}^-$  at the surface of the plane. A  $\text{pK}_a$  of 14 was chosen for CTAOH. The relevance of the choice for the  $\text{pK}_a$  of myristic acid is discussed below.

The dilute phase, if any, is modeled as a reservoir of uniform potential and ion concentrations. The system (reservoir + lamellar phase) is constrained by two conditions:

(i) Osmotic equilibrium between the dilute and the concentrated phases: the concentration  $c_i$  of all ionic species follows the law (uniform electrochemical potential for ion species),

$$c_i = c_i^{\text{res}} e^{-z(\varphi - \varphi^{\text{res}})/kT} \quad (1)$$

where  $c_i^{\text{res}}$  is the concentration of the ion in the reservoir,  $z$  its charge,  $\varphi^{\text{res}}$  the potential in the reservoir, and  $\varphi$  the potential at the position under consideration.

(ii) Global mass conservation: the compositions in water, surfactants, and  $X^-$  ions are set in the system. The volume fraction of the dilute phase  $F^{\text{dil}}$  and the water thickness  $D$  are therefore related by

$$1 - F^{\text{dil}} = \left(1 + \frac{D}{d}\right) \frac{1}{1 + \frac{\rho}{\rho_0} \left(\frac{1}{c} - 1\right)} \quad (2)$$

where  $d$  is the thickness of the lamellae,  $\rho$  and  $\rho_0$  the densities of the lamellae and water, and  $c$  the mass fraction of surfactant in the whole system. For the computations,  $d$  was set to  $43 \text{ \AA}$ ,  $c$  to 0.10,

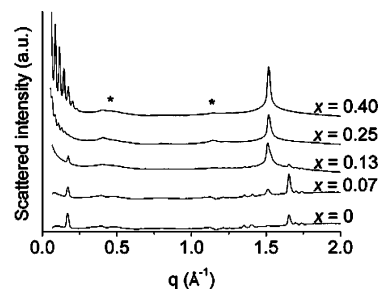


**Figure 1.** Typical WAXS patterns for catanionic mixtures of generic composition  $\text{C}_{13}\text{COOH}/\text{CTA}(\text{OH})_{1-x}\text{Cl}_x$ . For  $x = 0$  (bottom), characteristic peaks of a  $L_c$  phase are detected (e.g.,  $0.17$  and  $1.60 \text{ \AA}^{-1}$ ). For  $x = 0.40$  (top), the peaks of a swollen  $L_\beta$  lamellar gel phase are detected (up to eight 00*k* reflections for  $q < 0.30 \text{ \AA}^{-1}$ , and the 110 degenerated with the 020 at  $q = 1.52 \text{ \AA}^{-1}$ ). For intermediate ratios, both patterns are superimposed. The stars indicate a signal from the sample cell.

and  $\rho/\rho_0$  to 1. Additionally, the mean concentration of exchanged ions, which is imposed experimentally, must fulfill

$$\langle [X^-] \rangle = c_X^{\text{res}} \left( F^{\text{dil}} + (1 - F^{\text{dil}}) \frac{2}{D} \int_0^{D/2} e^{-z(\varphi - \varphi^{\text{res}})/kT} dx \right) \quad (3)$$

where  $x$  is the distance from the surface of a lamella.

During the computation,  $D$  and therefore  $F^{\text{dil}}$  are set to a given value. The Poisson–Boltzmann equation is then iteratively solved until the electrostatic potential profile, the surface charge densities, and the concentration of ions in the reservoir become self-consistent.

## Results and Discussion

**1. Phase Behavior of the Myristic Acid/CTA(OH)<sub>1-x</sub>Cl<sub>x</sub>/Water System.** The aim of this work is to study the effect of exchanging an  $\text{OH}^-$  ion with another anion in a myristate/cetyltrimethylammonium system. This can be performed either by introducing the conjugated acid HX or the salt CTAX in the preparation. Both methods are equivalent to using  $\text{CTA}(\text{OH})_{1-x}\text{X}_x$  as a cationic surfactant. In all preparations, we keep the myristic/CTA ratio equal to 1, and the mass concentration of myristic acid + CTA is kept equal to 10% weight. As expected, the use of CTAX, HX, or a mixture of both gave identical results. Note that above  $x = 1$ , all  $\text{OH}^-$  counterions are replaced with  $X^-$  counterions, and additional  $X^-$  anions are necessarily introduced as salt (or co-ions) together with  $\text{H}^+$ .

Typical WAXS patterns are reported in Figure 1 for various values of  $x$ . For  $x = 0$ , the pattern shows a series of sharp peaks characteristic of the powder pattern of a three-dimensional crystal (Figure 1, bottom). A single peak at  $q = 0.17 \text{ \AA}^{-1}$  is well apart from the other reflections, the latter being gathered at higher  $q$  values ( $1.35, 1.41, 1.65, 1.70$ , and  $1.74 \text{ \AA}^{-1}$ ). This clear separation is the signature of a crystallographic unit cell with a large aspect ratio.<sup>22</sup> The peak at  $q = 0.17 \text{ \AA}^{-1}$  is attributed to the 001 reflection, and the  $c$  parameter of the unit cell can be estimated to  $37 \text{ \AA}$ . As this coincides approximately with the double length of the surfactants, this pattern is attributed to a  $L_c$  phase. Those phases contain only a low content of water and are sometimes referred to as “collapsed lamellar phases”, although this term overlooks the 3D correlation and possible “head to tail” arrangements similar to the A-super form of fatty acids.<sup>23–25</sup>

(22) Vand, V. *Acta Crystallogr.* **1948**, *1*, 290.

(23) Goto, M.; Asada, E. *Bull. Chem. Soc. Jpn.* **1978**, *51*, 70.

(24) Kaneko, F.; Yamazaki, K.; Kitagawa, K.; Kikyo, T.; Kobayashi, M.; Kitagawa, Y.; Matsuura, Y.; Sato, K.; Suzuki, M. *J. Phys. Chem. B* **1997**, *101*, 1803.

(25) Yu, G.; Li, H.; Hollander, F.; Snyder, R.; Strauss, H. *J. Phys. Chem. B* **1999**, *103*, 10461.

(19) Zemb, T.; Taché, O.; Né, F.; Spalla, O. *J. Appl. Crystallogr.* **2003**, *74*, 2456.

(20) Ninham, B.; Parsegian, V. *J. Theor. Biol.* **1971**, *31*, 405.

(21) Ricoul, F.; Dubois, M.; Belloni, L.; Zemb, T.; André-Barès, C.; Rico-Lattes, I. *Langmuir* **1998**, *14*, 2645.

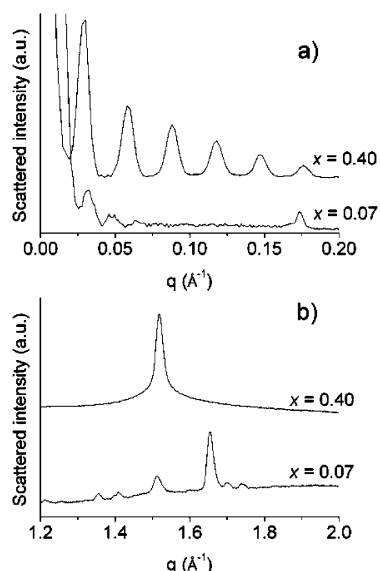


**Figure 2.** (a) SAXS patterns of catanionic mixtures of generic composition  $C_{13}COOH/CTA(OH)_{1-x}Cl_x$  with  $x = 0.07$  (bottom) and  $x = 0.40$  (top). (b) WAXS patterns in the region around  $q = 1.5 \text{ \AA}^{-1}$  of catanionic mixtures of generic composition  $C_{13}COOH/CTA(OH)_{1-x}Cl_x$  with  $x = 0.07$  (bottom) and  $x = 0.40$  (top).

For  $x = 0.40$ , the WAXS pattern shows major differences with the previous case (Figure 1, top). First, the peak at  $0.17 \text{ \AA}^{-1}$  is absent, demonstrating that no  $L_c$  phase is present anymore. Additionally, a series of Bragg peaks are observed at low  $q$ . They are attributed to the  $00k$  reflections of a lamellar phase. The separation between the peaks gives the repeating distance  $D^*$  between the lamellae, of the order of several hundreds of angstroms (see below). Up to 8 orders of diffraction are observed for these values of  $x$  by SAXS, indicating a well-defined smectic order with little fluctuations. Another characteristic feature of the pattern is the single peak at  $q = 1.52 \text{ \AA}^{-1}$ . This peak characterizes the in-plane correlation of the surfactant chains. The sharpness of the peak indicates that the chains are frozen<sup>26</sup> (thus the  $L_\beta$ ), as further confirmed by calorimetry and WAXS as a function of temperature.<sup>5,27</sup> This peak is unique, indicating that the in-plane arrangement of the surfactants is hexagonal.<sup>17,28</sup> It is therefore attributed to the 110 reflection, degenerated with the 020. Such a hexagonal arrangement of surfactants with frozen chains is characteristic of a gel phase in which the order in the chains is locally orthorhombic but is hindered by a large number of defects.<sup>29,30</sup>

For intermediate ion contents ( $0.07 < x < 0.20$ ), the peaks characteristic of the  $L_c$  phase are observed (Figure 1). In addition, a peak at  $1.52 \text{ \AA}^{-1}$  is also present, which characterizes the presence of surfactants bilayers with in-plane hexagonal arrangement (Figure 2b). The WAXS experiment resolves poorly the Bragg peaks in the low- $q$  region, and a similar SAXS setup with a higher sensitivity in the small  $q$  region reveals the presence of a series Bragg peaks (Figure 2a). Neutron scattering of samples prepared in deuterated water reveals also clearly the presence of these Bragg peaks in coexistence with the peak at  $0.17 \text{ \AA}^{-1}$  (Figure 4, bottom). The enhanced contrast to neutrons in the hydrogenated surfactants/deuterated water system allows a better

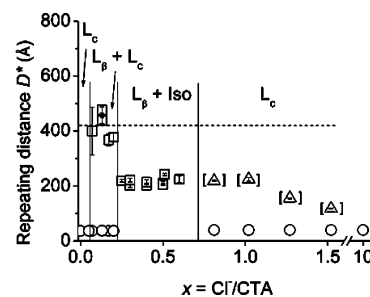


**Figure 3.** Summary of WAXS and SAXS data as a function of  $x$  in myristic acid/ $CTA(OH)_{1-x}Cl_x$  catanionic mixtures. The circles indicate the presence of  $L_c$  phase, arbitrarily set at the length of the lattice parameter  $c$ . The squares indicate the repeating distance of the  $L_\beta$  lamellar gel phase where it remains stable (i.e., over 6 months). The triangles indicate the transitory repeating distance measured after 4 weeks aging of the  $L_\beta$  gel phase where it is unstable. The horizontal dotted line indicates the approximate smectic distance for a pure  $L_\beta$  phase at this composition (10% weight surfactant).

discrimination of the smectic order than that achieved with the X-ray scattering experiments, where the water/surfactant electronic contrast is poor. It is however not excluded that a strong disorder between bilayers also occurs. At this composition in  $x$ , scattering studies therefore support that the  $L_c$  phase coexists with surfactant bilayers, showing hexagonal in-plane arrangement of surfactant chains, and that these bilayers are at least partially arranged into a  $L_\beta$  phase.

For any composition in  $x$ , the WAXS pattern corresponds to one of those three attributions: a three-dimensional  $L_c$  crystal, a swollen lamellar gel phase  $L_\beta$ , or a coexistence of  $L_c$  phase and bilayers arranged into a  $L_\beta$  phase. The nature of the phases was determined at constant surfactant concentration. Combination with SAXS experiments allows the repeating distance of the  $L_\beta$  phase, where it exists, to be accurately measured. These results are summarized together in Figure 3. With very little exchange of  $OH^-$  by other ions ( $x \leq 0.05$ ), only  $L_c$  crystals are observed. These crystals coexist with a water-rich phase. As the exchange ratio is increased ( $0.07 \leq x \leq 0.20$ ), the  $L_c$  phase coexists with bilayers with frozen chains at least partially arranged into a  $L_\beta$  phase. The relative amounts of  $L_c$  phase decreases as  $x$  increases, as demonstrated qualitatively by the changes in relative heights of the peaks at  $1.52$  and  $1.65 \text{ \AA}^{-1}$ . In this domain of composition, a pure  $L_\beta$  phase is transiently observed, but it rearranges within several weeks to yield the mixture of  $L_c$  and  $L_\beta$ . No further evolution was observed on the time scale of several months. The  $L_\beta + L_c$  coexistence indicates that, at these compositions, the interlamellar repulsions are too weak to stabilize completely the  $L_\beta$ . A collapse of one fraction of the lamellae allows the remaining fraction to be stabilized. This is generally driven either by a competition between attractive and repulsive interlamellar interactions or by demixion of the surfactants within the lamellae.<sup>31,32</sup> The collapsed lamellae then rearrange to yield the  $L_c$  phase. The remaining  $L_\beta$  phase shows a separation distance between lamellae of the order of  $400 \text{ \AA}$ , as determined from the separation of the Bragg peaks either in the X-ray or neutron scattering experiments (Figures 2a and 4).

At larger exchange ratios ( $0.20 \leq x \leq 0.60$ ), no  $L_c$  is observed anymore, but only  $L_\beta$ . This indicates that the repulsions between lamellae become strong enough to stabilize the lamellar phase, with a repeating distance  $D^*$  determined from the position of the Bragg peaks being remarkably independent of the amount of

(26) Tardieu, A.; Luzzati, V.; Reman, F. *J. Mol. Biol.* **1973**, *75*, 711.

(27) Vautrin, C.; Zemb, T.; Schneider, M.; Tanaka, M. *J. Phys. Chem. B* **2004**, *108*, 7986.

(28) Kitaigorodskii, A. In *Organic Chemical Crystallography*; Consultants Bureau: New York, 1961.

(29) Sirota, E. *Langmuir* **1997**, *13*, 3849.

(30) Sackmann, E. In *Structure and Dynamics of Membranes*; Lipowsky, R., Sackmann, E., Eds.; Elsevier Science B.V.: Amsterdam, 1995; Chapter 5.

(31) Dubois, M.; Zemb, Th.; Fuller, N.; Rand, R. P.; Parsegian, V. *J. Chem. Phys.* **1998**, *108*, 7855.

(32) Noro, M.; Gelbart, W. *J. Chem. Phys.* **1999**, *111*, 3733.



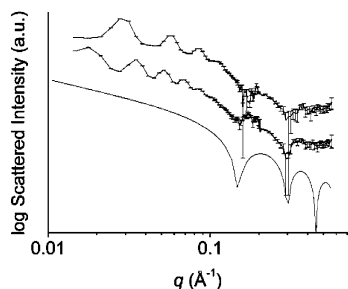


**Figure 4.** Small-angle neutron scattering of myristic acid/CTA(OH)<sub>1-x</sub>Cl<sub>x</sub> catanionic mixtures prepared in D<sub>2</sub>O. Top:  $x = 0.40$ . Bottom:  $x = 0.13$ . Full line: form factor of an infinite plate of thickness of 42 Å.

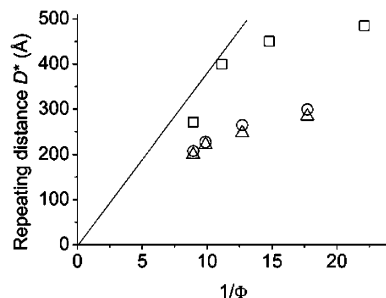


**Figure 5.** Dilution curve of myristic acid/CTA(OH)<sub>1-x</sub>X<sub>x</sub> catanionic mixtures. Straight line: expected for a monophasic L<sub>β</sub> phase with no water-rich phase. Circles and triangles: experimental data for X = Cl,  $x = 0.3$  and  $0.4$ , respectively. Squares: X = Br,  $x = 0.27$  with a fresh sample. The density of the bilayer was assumed to be 1.

counterions  $x$  ( $D^* \sim 215$  Å). The repeating distance of a pure, defect-free L<sub>β</sub> phase may be estimated from the bilayer thickness and the volume fraction of surfactant from

$$D^* = \frac{d}{\Phi} \quad (4)$$

From the concentration of surfactants (10% weight) and the thickness of the bilayer ( $\sim 42$  Å, Figure 4, see discussion below), and assuming a bilayer density close to 1, the theoretical maximum swelling of the L<sub>β</sub> is 420 Å. This value, indicated by the dotted line in Figure 3, is twice as large as the value experimentally measured. This is a first indication that the L<sub>β</sub> coexists with a water-rich phase.

More formal evidence is obtained by plotting the repeating distance  $D^*$  against the inverse volume fraction  $1/\Phi$  for different water contents (Figure 5). If all the water swells the lamellar phase, a linear dependence is expected, with the slope giving the thickness  $d$  of the bilayer. Any deviation from a linear swelling toward an asymptote detects the coexistence of the lamellar phase with another phase competing for water, usually unilamellar vesicles. The absence of swelling allows a phase limit to be detected.<sup>33</sup> A linear dependence is detected for instance with  $X^- = \text{Br}^-$ ,  $x = 0.27$  at surfactant volume fractions above 9%. In the present case of  $X^- = \text{Cl}^-$  and  $0.20 < x < 1$ , no such linear dependence is observed. This demonstrates that the L<sub>β</sub> phase coexists with a water-rich phase at the concentration under investigation. Equation 2 gives an approximation for the volume fraction of dilute phase in the sample, assuming that the amount of surfactant is negligible in the dilute phase. If the density of the lamellae is assumed to be 1, the volume fraction of the dilute phase in the sample is found to be 40%. It means that only 55% of the water is retained in the lamellar phase.

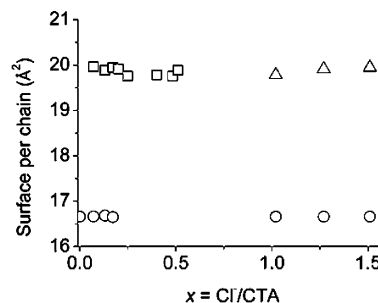


**Figure 6.** Surface per chain in myristic acid/CTA(OH)<sub>1-x</sub>Cl<sub>x</sub> catanionic mixtures. For the sake of clarity, circles are plotted at a surface of 17 Å<sup>2</sup> where L<sub>c</sub> crystals are detected. Squares indicate experimental values for the L<sub>β</sub> phase as determined by the WAXS measurements. Triangles indicate the values for a transient L<sub>β</sub> phase measured after 4 weeks of aging.

As  $x$  is further increased, L<sub>c</sub> crystals are again observed ( $x \geq 0.80$ ). The L<sub>β</sub> phase is transiently detected, but vanishes with time scales varying from days ( $x = 10$ ) to months ( $x = 0.80$ ). The repeating distance  $D^*$  of the transient L<sub>β</sub> is decreasing with time, until the L<sub>β</sub> completely vanishes. At these ratios, the increase of  $x$  necessarily introduces co-ions in the preparation in the form of HCl. It seems intuitive to attribute the progressive collapse of the L<sub>β</sub> phase to the screening of the charges. It is less intuitive that this “screening” occurs even at  $x$  values below 1, for which no excess HCl is normally present. As detailed below, the osmotic pressure of the ions expelled into the dilute phase accounts at least partially for this early destabilization.

**2. Structure of the Bilayers.** This sequence of phases observed at a colloidal scale contrasts with the total absence of in-plane structural changes in the bilayer of the L<sub>β</sub> phase. Small-angle neutron scattering of the catanionic mixtures prepared in D<sub>2</sub>O allows the thickness of the bilayer to be determined from the form factor in different phase domains (Figure 4). The oscillations in the small  $q$  range are Bragg peaks attributed to the plane–plane correlations and coincide well with those measured by SAXS at the same composition. For the composition  $x = 0.13$ , the peak at  $0.17$  Å<sup>-1</sup> originating from the L<sub>c</sub> phase is also present. By contrast to X-ray experiments, additional oscillations are observed around  $0.15$  and  $0.30$  Å<sup>-1</sup>. They are attributed to the first two minima of the form factor of the bilayer. Comparing the medium-to-high  $q$  range part of the curve with the theoretical form factor of a plate of infinite extension allows the thickness of the bilayer to be estimated at 42 Å. It is observed that the thickness of the L<sub>β</sub> bilayer is identical in the L<sub>c</sub> + L<sub>β</sub> domain and in the L<sub>β</sub> domain, although the smectic distance varies by a factor of 2, as shown by the position of the Bragg peaks.

Additionally, the surface per surfactant chain can be measured from the position of the 110 peak on the WAXS pattern:

$$S = \frac{2}{\sqrt{3}} \left( \frac{2\pi}{q_{110}} \right)^2 \quad (5)$$

The surface per surfactant was found to be nearly constant and remains around 20 Å<sup>2</sup> for all the samples investigated (Figure 6). It demonstrates that the driving force for the out-of-plane stabilization of the layers, discussed below, has very little influence on the in-plane packing of the adjacent crystallized chains.

**3. Effect of the Nature of the Ion.** This response to ion exchange, extensively described for the introduction of Cl<sup>-</sup>, was also examined with other anions (acetate, bromide, and tosylate). The most systematic effects were observed at intermediate exchange ratios ( $0.20$ – $0.40 < x < 1$  depending on the anion).

(33) Dubois, M.; Zemb, T. *Langmuir* **1991**, *7*, 1352.

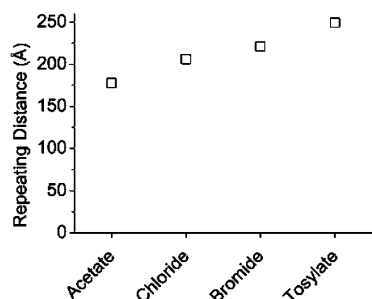


**Figure 7.** Repeating distances of the  $L_\beta$  phases at  $x = 0.50$  for various  $X$  anions. All samples are in a  $L_\beta + \text{Iso}$  domain.

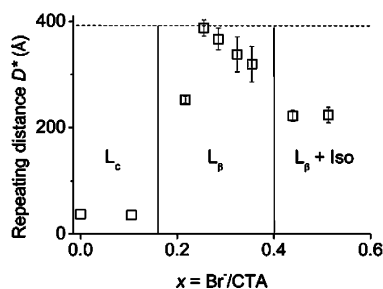


**Figure 8.** Summary of WAXS and SAXS data as a function of  $x$  in myristic acid/CTA(OH) $_{1-x}$ Br $_x$  catanionic mixtures. The circles indicate the presence of  $L_c$  phase, arbitrarily set at the length of the lattice parameter  $c$ . The squares indicate the repeating distance of the  $L_\beta$  lamellar gel phase where it exists. The horizontal dotted line indicates the approximate smectic distance for a pure  $L_\beta$  phase at this composition (10% weight surfactant).

In this regime, the myristic acid/CTA(OH) $_{1-x}$ X $_x$ /water mixtures form a  $L_\beta$  phase in coexistence with a water-rich phase, with a repeating distance again independent of  $x$ , but dependent on the nature of the anion under inspection (Figure 7). The swelling  $D^*$  increases in the sequence acetate < chloride < bromide < tosylate. This ion sequence follows the Hofmeister series from the more dissociated (cosmotropic) to the more associated (chaotropic) ions.<sup>34</sup> Another remarkable effect of the nature of the ion is the quenching of the  $L_\beta$  to  $L_c$  transition at low  $x$ . For the chloride ions, a transient pure  $L_\beta$  phase is observed before the  $L_\beta + L_c$  coexistence is observed at  $0.05 < x < 0.20$ . The same behavior is observed with acetate ions, but for the most hydrophobic ions (bromide and tosylate), this transition is not observed within time scales of several (>6) months (Figure 8). It is not clear yet whether this effect is thermodynamic or kinetic, but it still demonstrates the relevance of the nature of the ions in such catanionic mixtures.

**4. Force Balance.** The main trends of the above experimental results can be summarized as follows: in the myristic acid/CTA(OH) $_{1-x}$ X $_x$ /water mixtures, a pure  $L_\beta$  phase in coexistence with water is observed only in a narrow domain of composition in  $X^-$ . In this domain, the repeating distance of the  $L_\beta$  is remarkably stable against the ratio  $x$ . Otherwise, if the amount of exchanged ions is too small, or too large, the crystalline  $L_c$  phase is observed, which may transiently coexist with the  $L_\beta$  phase. These experimental observations can be qualitatively interpreted in terms of interlamellar repulsions.

For this purpose, we use a model where the forces of electrostatic nature between the lamellae are computed numerically. The system is modeled as a stack of charged lamellae in thermodynamic equilibrium with a dilute phase of finite volume. The inputs in the model are the interlamellar distance, the global

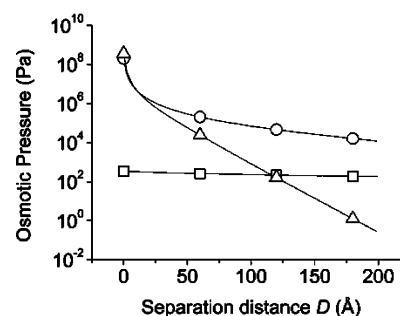


**Figure 9.** Osmotic pressure as a function of the separating distance between two myristic acid/CTA(OH) $_{1-x}$ X $_x$  plates in coexistence with excess water from a Poisson–Boltzmann model with charge regulation and imposed overall composition ( $c = 10\%$  weight).  $pK_a = 6.3$  for myristic acid,  $pK_a = 14$  for CTAOH. Squares:  $x = 0$ . Circles:  $x = 0.50$ . Triangles:  $x = 1.25$ .

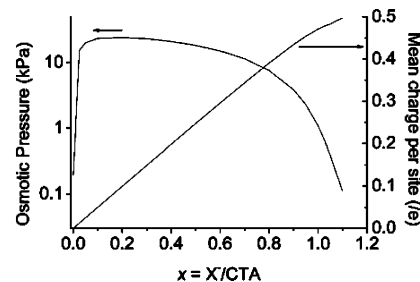


**Figure 10.** Electrostatic pressure (left axis) and mean surface charge per site (right axis) between two myristic acid/CTA(OH) $_{1-x}$ X $_x$  plates in coexistence with excess water from a Poisson–Boltzmann model with charge regulation and imposed overall composition ( $c = 10\%$  weight), separated by a distance of  $D = D^* - d = 173$  Å.  $pK_a = 6.3$  for myristic acid and  $pK_a = 14$  for CTAOH.

composition (in surfactant, water, and  $X^-$  ions) and the  $pK_a$ 's for both surfactants. In this closed system, the work to move apart the lamellae equals the work required to transfer water molecules from the dilute phase to the concentrated phase, at constant total volume. The electrostatic contribution to the pressure between the planes is therefore

$$\pi^{\text{elec}} = kT \sum_{\text{ions}} (c_i^{\text{mid}} - c_i^{\text{res}}) \quad (6)$$

where  $c_i^{\text{mid}}$  is the concentration of the ion  $i$  at the midplane of the lamellae. There are two opposite contributions to the electrostatic pressure between the lamellae: a positive contribution from the pressure of the ions between the lamellae and a negative contribution arising from the osmotic stress from the ions in the dilute phase. As illustrated below, the latter may become far from negligible.

The first striking experimental observation is that the  $L_\beta$  phase is present only in a narrow domain of composition in  $X^-$  ions. This behavior is well-described by the Poisson–Boltzmann model, which predicts a maximum in the electrostatic pressure at a given distance as  $x$  varies. In the absence of  $X^-$  ions, the electrostatic repulsions between two  $L_\beta$  planes are predicted to remain extremely weak even at the shortest distances (<250 Pa, Figure 9). A detailed analysis of the calculations shows that both surfactants are fully dissociated, yielding a zero surface charge density at  $x = 0$  (Figure 10). As the respective counterions are  $H^+$  and  $OH^-$  only, the concentration of ions in the interlamellar space is limited by the self-dissociation of water, which allows very short separation distances with no significant increase in the osmotic pressure. In the absence of other repulsive interactions, any existing  $L_\beta$  phase would therefore collapse for  $x = 0$ .

(34) Kunz, W.; Lo Nostro, P.; Ninham, B. *Curr. Opin. Colloid Interface Sci.* **2004**, *9*, 1.

By contrast, the interlamellar repulsions are predicted to increase dramatically as  $x$  is set to nonzero values (Figure 9), resulting from the increase in the charge of the lamellae (Figure 10). At short distances, the electrostatic pressure is dominated by the first term in eq 4. The concentration of ions at the midplane scales as  $x/D^*$  and the pressure is found to diverge to infinite at short distances. This correlates well with the experimental observations, which show the stability of the  $L_\beta$  phase in a narrow domain of composition ( $0.2 \leq x \leq 0.6$ ), first in coexistence with and then in the absence of  $L_c$ . Another experimental observation of interest in this domain is the striking stability of the repeating distance. This contrasts with the prediction for the electrostatic interactions at  $D^* = 215$  Å (Figure 10): assuming a  $pK_a$  value of 6.3 for myristic acid as measured for fatty acids inserted into surfactant micelles,<sup>35</sup> the electrostatic pressure is expected to decay from 24 kPa at  $x = 0.2$  to 12 kPa at  $x = 0.7$ . This is counterintuitive, as the mean charge per site is continuously increasing as  $x$  increases. The origin of such decay is the competition between the osmotic pressure between the planes and in the dilute phase (eq 4). The first term dominates at small  $x$  values, and the repulsion at a given distance is found to increase steeply as the lamellae get positively charged. As  $x$  further increases, the negative contribution becomes relevant and the electrostatic pressure is predicted to decrease despite the increase in the charge of the lamellae. This decrease occurs before any excess salt is present in the solution ( $x = 1$ ). This is a consequence of a partial transfer of ions from the interlamellar space to the dilute phase. This amount is extremely small: for example, only 4% of the chloride ions are released from the interlamellar space at  $x = 0.5$ . This is however enough for the electrostatic repulsion to become significant (eq 4), with a concentration of chloride ions of 0.232 M at the midplane vs a concentration of 0.097 M in the dilute phase.

Despite a decrease by a factor of 2 in the electrostatic repulsions, the repeating distance was found to be remarkably stable, which means that the force balance must compensate exactly for this variation. The van der Waals interactions are found to be negligible:

$$\pi^{\text{vdW}} = -\frac{A}{6\pi} \left( \frac{1}{D^3} - \frac{2}{(D+d)^3} + \frac{1}{(D+2d)^3} \right) < 20 \text{ Pa}$$

for a typical Hamaker constant of  $6 \times 10^{-21} \text{ J}^{36}$

Helfrich repulsions can also be safely ruled out as expected for stiff  $L_\beta$  phases: from the measured bending rigidity of the walls ( $\kappa = 450 k_B T$ )<sup>37</sup> and the in-plane persistence length from cryofracture measurements ( $\xi > 1 \mu\text{m}$ ),<sup>4</sup> one can estimate the order of magnitude of the disjoining pressure of entropic origin:<sup>38</sup>

$$\pi^{\text{Helf}} \approx \frac{\sqrt{\kappa k T}}{\xi^3} < 0.1 \text{ Pa}$$

Finally, the only remaining force of relevance is the pressure originating from the osmotic equilibrium between the  $L_\beta$  phase and the water-rich phase. In binary mixtures of glycolipids and DDAB, it has been demonstrated that this force accounts for

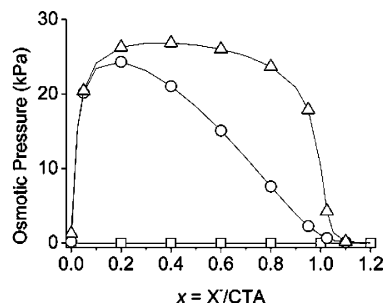


**Figure 11.** Electrostatic pressure between two myristic acid/CTA-(OH)<sub>1-x</sub>X<sub>x</sub> plates in coexistence with excess water from a Poisson–Boltzmann model with charge regulation and imposed overall composition ( $c = 10\%$  weight), separated by a distance of  $D = D^* - d = 173$  Å.  $pK_a = 14$  for CTAOH and  $pK_a = 0$  (squares),  $pK_a = 6.3$  (circles), and  $pK_a = 9$  (triangles) for the anionic surfactant.

the depletion of a lamellar phase by a micellar phase.<sup>39</sup> This very general mechanism sets the maximum swelling of lamellar phases in coexistence with dilute phases. Here, the remarkable stability of the smectic distance as  $x$  varies indicates that the osmotic pressure in the dilute phase must show exactly the same variations as the electrostatic pressure in the lamellar phase.

For  $x$  values above 0.80, the model predicts a drastic decrease in the interlamellar repulsions (Figure 9 and Figure 10). This is in agreement with the experimental observations, which demonstrate the instability of the  $L_\beta$  phase at  $x \geq 0.80$ . According to the Poisson–Boltzmann model, the planes almost reach the maximum charge density achievable ( $+1/2e$  per site, Figure 10), but this is now largely compensated by the negative term in eq 4.

Most of the experimental observations we report here on the myristic acid/CTA(OH)<sub>1-x</sub>X<sub>x</sub>/water system can be qualitatively described in terms of electrostatic interactions. Considerations about the osmotic pressure of the ions between the interlamellar space and the dilute phase give a satisfying qualitative description of the system, i.e., stabilization of the  $L_\beta$  phase in a narrow domain of composition of  $X^-$ . However, an accurate inspection of the dilute phase is necessary to understand the details of osmotic equilibrium that allows the repeating distance to remain so insensitive to the ion content. In addition, the choice of the  $pK_a$  values, in particular for the anionic surfactant, may be discussed. In the range  $2 \leq pK_a \leq 7$ , the predictions from the model are not qualitatively changed: at any given distance, a maximum in the electrostatic pressure is found in a narrow range of composition in  $x$ . The  $pK_a$  value of 6.3 we have used in Figure 10 may be discussed, as the  $pK_a$  of fatty acids is known to be significantly altered by the local environment (dielectric interface, packing, etc.).<sup>26,40,41</sup> However, it does not change qualitatively the main outcome, which is the existence of the narrow domain of stability if the acid is weak enough. If the anionic surfactant is a strong acid, the lamellae are predicted to be always unstable (Figure 11). The addition of HCl cannot reduce the dissociation of the anionic surfactant, and the charge remains too weak to induce any significant electrostatic pressure. By contrast, if the anionic surfactant is a very weak acid, the lamellae are more easily charged, which both increase the positive term and decrease the magnitude of the negative term in eq 4. The domain of stability of the catanionic mixture is then predicted to be broader with a weaker acid (Figure 11).

(35) Whiddon, C.; Bunton, C.; Söderman, O. *J. Phys. Chem. B* **2003**, *107*, 1001.

(36) Parsegian, V. A. In *Van der Waals forces*; Cambridge University Press: New York, 2006.

(37) Delorme, N.; Dubois, M.; Garnier, S.; Lachewsky, A.; Weinkamer, R.; Zemb, T.; Fery, A. *J. Phys. Chem. B* **2006**, *110*, 1752.

(38) Lipowski, R. In *Structure and Dynamics of Membranes*; Lipowski, R., Sackmann, E., Eds.; Elsevier Science B.V.: Amsterdam, 1995; Chapter 11.

(39) Ricoul, F.; Dubois, M.; Zemb, T.; Plusquellec, D. *Eur. Phys. J. B* **1998**, *4*, 333.

(40) Bunton, C.; Minch, M. *J. Phys. Chem.* **1974**, *78*, 1490.

(41) Fernandez, M.; Fromherz, P. *J. Phys. Chem.* **1977**, *81*, 1755.

### Conclusion

Equimolar mixtures of myristic acid and hexadecyltrimethylammonium hydroxide (CTAOH) usually form  $L_c$  phases. However, exchange of  $OH^-$  anions with other  $X^-$  anions of any nature allows a swollen  $L_\beta$  phase in coexistence with a water-rich phase to be stabilized. This stabilization occurs on a narrow domain of composition. In this domain, the amount of  $X^-$  anions does not influence the interlamellar distance  $D^*$ , nor their in-plane structure. However, more structure-breaking (hydrophobic, chaotropic) anions increase the swelling of the phase. The Poisson–Boltzmann model with charge regulation and imposed overall composition in the lamellar phase + excess water predicts qualitatively the stability of the  $L_\beta$  phase in a small domain of

composition in  $X^-$  anions and relates the width of this domain to the  $pK_a$  of the surfactants used in the catanionic mixture. This understanding of the stabilization of lamellar gel phases as an ion pair amphiphile is turned into a surfactant mixture opens new perspectives in the design of self-assembled catanionic structures, especially in domains of composition where their stabilization is difficult to achieve.

**Acknowledgment.** The authors thank the European Master “Complex Condensed Materials and Soft Matter” (EMASCO-COSOM).

LA070184W